Chapter 4

Design Aspects of Capacitor Banks for Pulsed Power Applications

—Dr. Rishi Verma

Capacitive energy storage is widely used in various pulsed power applications but the intricacies in achieving higher-end performance depends on major factors like selection of appropriate type of capacitors and switches, their integration approach and mode of load connection. The inherent characteristics and ratings of constituting components of capacitor bank majorly determine the amplitude and temporal response of output current pulse. This chapter comprehensively elaborates contemporary and novel options adopted by practicing engineers and provides methodical guidance on judicious selection of appropriate component and implemented configuration that may be best suited for an application.

4.1. Introduction

The range of applications of high current capacitor banks is extensive covering industrial, defense and scientific applications like pulsed electromagnetic welding [1], shockwave generation [2], neutron generation [3], Z-pinch driven inertial fusion [4], electromagnetic launchers [5] *etc.* Each of these applications requires different amplitude, frequency and duration of pulsed current discharge and hence tailoring of driving pulse becomes mandatory.

The primary objective of building capacitor banks is to source large magnitude of peak current ranging from few 10's of kA to few MA for the durations of few hundreds of nanoseconds to milliseconds. The simplified electrical equivalent of a typical capacitor bank is an LCR series circuit that determines the output pulse characteristics. Schematic shown in Figure 4.1, C_o is total capacitance of a capacitor bank charged to voltage V_o, and L_o and R_o are the equivalent circuit inductance and resistance, respectively.

After closing the switch, energy of capacitor bank discharges and current that flowing through the load is:

$$I(t) = (V_0/\omega L_0)e^{-\alpha t} Sin\omega t \tag{4.1}$$

Here, $\alpha = R_0/2L_0$; $\omega = \sqrt{\dfrac{1-r^2}{L_0C_0}}$ with $r = \sqrt{\dfrac{R_0C_0}{4L_0}}$

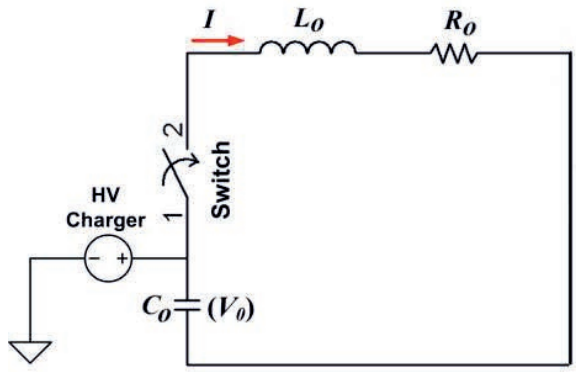

Figure 4.1. Electrical schematic of capacitor bank.

The resistance (R_0) of electrical circuit is normally low (~mΩ) and the capacitors also have low equivalent series resistance, under such conditions peak current (I) and the time period (T) of discharge signal is approximated as:

$$I = V_0\sqrt{\frac{kC_0}{L_0}} \tag{4.2}$$

$$k = e^{-\pi r/\sqrt{1-r^2}} \tag{4.3}$$

$$\left(\frac{dI}{dt}\right) = \frac{V_0}{L_0} \tag{4.4}$$

$$T = \frac{2\pi}{\omega} = 2\pi\sqrt{L_0C_0} \tag{4.5}$$

Here, the ratio of peaks in each discharge cycle is defined as voltage reversal factor *k*. It can be seen from equation nos. 4.2, 4.3 and 4.4, to obtain larger amplitude of peak discharge current *I* and maximum *dI/dt* the overall inductance L_o and resistance R_o in the circuit must be very low. A simple expression that is utilized for the estimation of charge transfer (Q) in a typical under-damped circuit response (as shown in Figure 4.2) is given as:

$$Q = \frac{T}{\pi} \times \frac{I_{pk}}{(1-k)} \tag{4.6}$$

Here, the voltage reversal factor k is calculated by using the expression:

$$k = \frac{1}{n-1}\left(\frac{V_2}{V_1} + \frac{V_3}{V_2} + \text{.....} + \frac{V_n}{V_{n-1}}\right) \tag{4.7}$$

Equivalent resistance of under-damped LCR circuit is determined from expression:

$$R_o = -\frac{2}{\pi}\sqrt{\frac{L_0}{C_0}}\ln k \tag{4.8}$$

The major hardware components of capacitor banks and aspects concerning design and application are detailed in further sections.

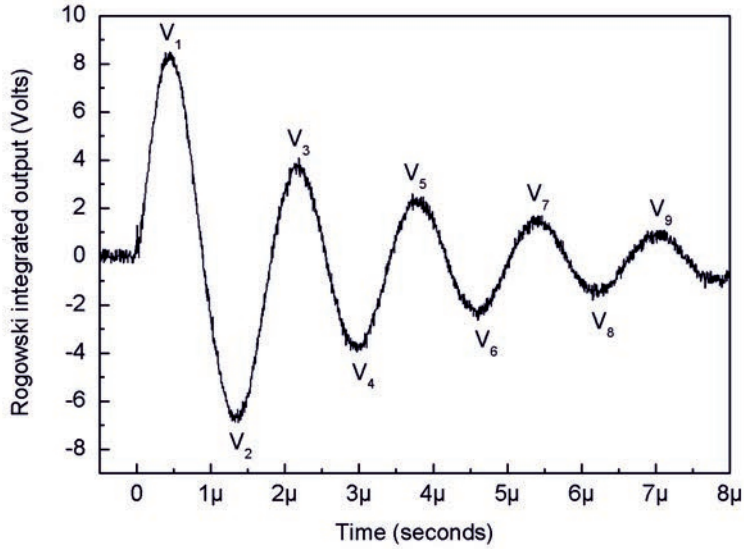

Figure 4.2. Sample trace of an under-damped circuit response.

4.2. Capacitors for Pulsed Power

The distinctive features of capacitors being used for energy storage purpose in a pulsed power system are their capability of delivering large peak current, having low series inductance (ESL) and low resistance (ESR), high voltage withstand capacity and they perform very reliably under large electrical stress. Figure 4.3 shows the electrical equivalent of capacitor.

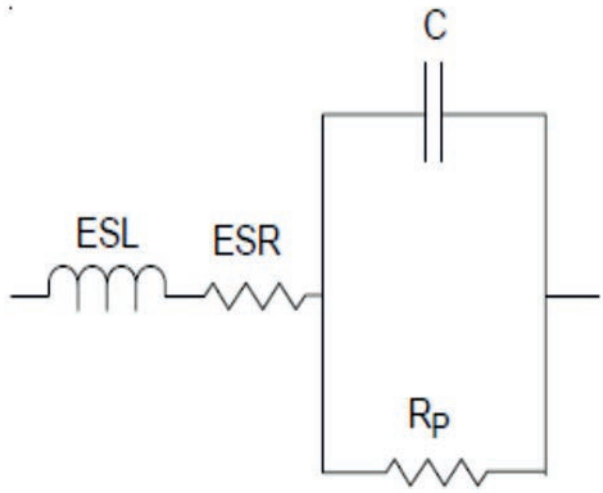

Figure 4.3. Electrical equivalent of energy storage capacitor.

Fundamental equations that determine the discharge characteristics of capacitor are,

$$C = \frac{\varepsilon_o KA}{d}; \tag{4.9}$$

$$\frac{di}{dt} = \frac{V_o}{ESL} \tag{4.10}$$

$$ESR = \frac{DF}{\omega C} \tag{4.11}$$

The major elements of an energy storage capacitor is conducting foil/film, intermediate dielectric and insulating fluid. Interleaved sheets of the conducting foil/film and dielectric film immersed in insulated medium constitutes an Energy Storage Capacitor (ESC). From Eq. (4.9) it is clearly evident that capacitance is largely dominated by the choice of dielectric material (having dielectric constant K) and its thickness d that creates separation between the metal foil/plates. It is remarkable to note that larger is the dielectric constant K and electrical breakdown strength E of insulating layer (so that minimum thickness of inter-layers can be used), higher is constructional energy density of capacitor resulting in its smaller size. This relation is depicted in Eq. (4.12) [6].

$$U = \frac{1}{2} . \varepsilon_o . \varepsilon_r . E^2 . PF . 10^6 \tag{4.12}$$

Here, U denotes energy density (J/cc), ε_o is free space permittivity (8.85×10^{-12} F/m), $\varepsilon_r$is relative permittivity, E is electric field in V/µm and PF is the packing factor.

Construction wise capacitors in pulsed power applications are broadly of three types: paper-foil; film-foil and metalized-film. In the paper-foil and film-foil capacitors a thin aluminum foil electrode of about 5.5 µm is used along with paper/polypropylene film as dielectric layer where as in metalized-film capacitors electrode is aluminum/zinc metal vapour of about 0.025 µm that is directly deposited on the dielectric layer. The typical thickness of dielectric film used in various combinations varies in the range of 12 µm to 60 µm.

Owing to about 200 times lesser electrode thickness than aluminum foil, metalized electrode capacitors have very high energy density (because PF enhances multifold) but performance wise they suffer with following limitations: (i) large peak currents cannot be drawn due to higher surface resistivity (ii) the end connections of metalized electrodes are the weak links in this type of capacitor construction. (iii) not suitable for use in fast discharge applications (at high frequency the resistance dominates and the ESR/DF becomes significantly high).Metalized capacitors are best suited for high energy density, slow discharge, low peak current applications for e.g. electromagnetic launchers and medical defibrillator. It's worth noting that till date oil impregnated craft paper-aluminum foil capacitors are most robust, deliver large peak currents and able withstand large voltage reversal.

In the past years there has been large thrust towards improvement in energy density of capacitors that are regularly used in various pulsed power applications. A brief summary of advancements in this direction is summarized in Table 4.1.

Table 4.1. Typical energy densities of various construction technologies used in ESC.

Generation	**Construction technique**	**Energy density**	**Shot-life '*n*'**
1st Generation	Paper & Foil	0.4 J/cc	5
2nd Generation	Paper + PP film & Foil	1 J/cc	7 to 9
3rd Generation	Paper + PP film & Metalized electrode	1.5 J/cc	15
4th Generation	PVDF & Metalized electrode	2.4 J/cc	15

Poly-Vinyli-Dene Fluoride (PVDF) is a new dielectric material that is biaxial oriented film and upon polarization forms the basis of piezoelectric and pyroelectric devices. Its high dielectric constant (~12) results in energy density of about 2.4 J/cc. Even though PVDF offers highest dielectric constant and energy density, but its drawbacks are: (i) instability in the dielectric constant (varies considerably with voltage, temperature and frequency) (ii) very low insulation resistance (iii) low self-healing ability (iv) leakage current is high and breakdown at lower voltages (v) poor mechanical properties (vi) getting uniform thickness and thin gauge sheet is difficult (vii) expensive due to limited availability. The typical properties of various dielectric materials used in construction of energy storage capacitors are summarized as under:

Table 4.2. Properties of various dielectrics used in capacitor construction.

Dielectric	***K***	**E (V/μm)**	**DF (%)**	**ρ (ohms-cm)**	**T (°C)**
Kraft Paper	4-6	160	<0.005	3×10^{16}	85
Polypropylene (PP)	2.2	500	<0.1	1×10^{18}	105
Polyester (PET)	3.3	400	<1.5	1×10^{17}	125
Poly-Vinyli-Dene Fluoride (PVDF)	12	200	1-5	1×10^{15}	105

For replacing air spaces between layers of wounded dielectric and electrode, dielectric fluid is filled inside the capacitor. The addition of dielectric fluid decreases the high voltage stress and increases breakdown strength of inter-layer. The most commonly used liquids in capacitors are Castor oil, Jarylec, SAS-60E and Phenyl Xylyl Ethane (PXE).

Capacitors are the most important and expensive hardware and its choice is conciliation between cost, performance and life expectancy/ shot life. Shot life (Λ) of capacitor is dictated by two important factors:

(i) Capacitor charging voltage (V_o) and

(ii) Voltage reversal factor (k)

Shot life of a pulse discharge capacitor is empirically predicted as [7]:

$$\Lambda_{op} = \Lambda_r \times \left[\frac{\omega_r}{\omega_{op}}\right]^{1.6} \times \left[\frac{V_r}{V_o}\right]^n \tag{4.13}$$

Here Λ, V and ω represent shot-life, capacitor charging voltage and ringing factor respectively for the rated (r) and operating (op) conditions. In this formula exponent 'n' represents the shot life scaling factor that has been established for various construction techniques. Its values for various dielectric combinations are shown in Table 4.1. The relationship between voltage reversal and ringing factor is mentioned as under [7]:

$$\omega = \sqrt{1 + \frac{1}{\left[\frac{2}{\pi}\ln(k)\right]^2}} \tag{4.14}$$

In Eq. (4.13), exponent 'n' is typically around 7.5 and thus charging voltage is the most important life deciding factor. Low charging voltage improves the shot life of capacitors. By operating at ~50% of rated voltage, shot life gets increased by factor of ~1000 [8]. Voltage reversal factor (k) with 1.6 as exponent also effects the shot life of capacitor, particularly with under damped (ringing) discharges; large internal stresses are generated on components. It is typically in the range of $0 < k < 1$. It shall be noted that cost of the capacitor scales-up with each 10× scaling in its shot life. The estimation of exemplary degradation in shot life of 0.3 µF/30 kV capacitor with Paper + PP film & Foil construction having rated shot life of 10^8 shots at 20% voltage reversal is shown below in Figure 4.4. Shot life typically reduces by 100 times if the same capacitor is used at 90% voltage reversal.

4.3. Switching

A triggerable switch is incorporated in capacitor bank to rapidly transfer its stored energy into the load. There is a wide range switches used in pulsed power systems are – Sparkgap, Railgap, Ignitron, Pseudospark etc. Required switching performance is the major criteria for selecting a particular switch type. There is always a trade-off between cost, complexity in triggering, and jitter in switching. Main factors to be considered when choosing a suitable switch are (a) voltage retention range (b) peak current capacity (c) inductance and (d) switch lifetime.

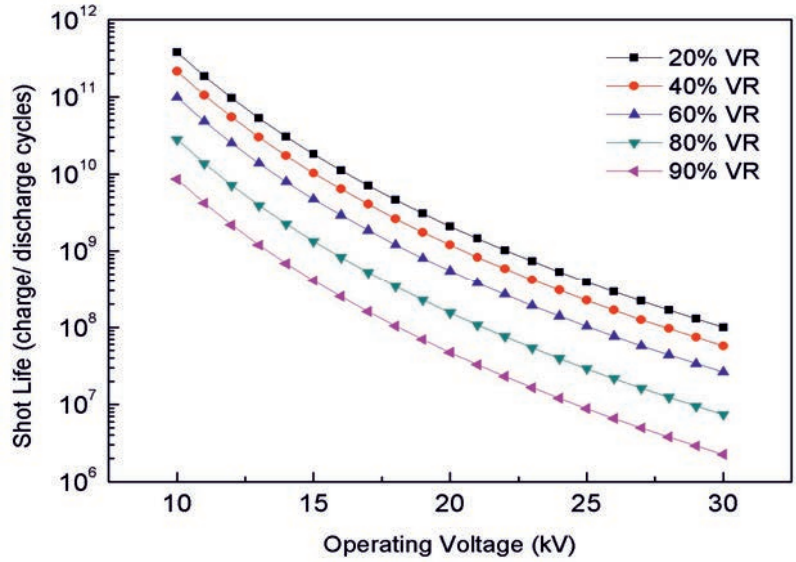

Figure 4.4. Life expectancy of capacitors at higher voltage reversals.

4.3.1. Spark-gap Switch

Pressure-triggerable spark gaps are technically viable and economic due to their simple design, low inductance, simple triggering, and ease of use. The breakdown voltage V_{bd} for a spark gap is mainly the function of gas pressure p (in bar) and the inter-electrode gap d (in cm) and is expressed as [9, 10].

$$V_{bd} = 24.4pd + 6.53\sqrt{pd} \tag{4.15}$$

The basic physical mechanisms that cause high voltage breakdowns in spark gap switches have been extensively studied by many researchers [11-14], and the cause of breakdown / conduction delay is accredited on three factors i.e. Statistical (t_s), formative (t_f), and channel heating time (t_{ch}). Switching jitter largely depends on statistical time lag [10].

$$t_{bd} = t_s + t_f + t_{ch} \tag{4.16}$$

Statistical lag (t_s) is the average duration for an electron to appear in inter-electrode region so that breakdown may be initiated. Formative lag (t_f) is the duration in which ionization grows and weekly ionized plasma is formed. Formative time lag is inherently reduced at higher operating voltages. Channel heating time(t_{ch}) is the time interval during which the impedance/voltage across the sparkgap starts collapsing and plasma channel becomes fully conducting. The empirical relation between time delay, electric field in main gap and fill gas pressure as follows [15]:

$$\rho\, t_{bd} = 97800\left(\frac{E}{\rho}\right)^{-3.44} \tag{4.17}$$

Here, ρ in g/cm^3 is the gas density, t_{bd} in seconds is the breakdown time and E is mean electric field in kV/cm. From the above relationship, we can see that the breakdown time strongly depends on applied voltage to the switch. The triggerablesparkgap switches mainly have three configurations (i) Trigatron (ii) Field distortion and (iii) Laser triggered. The fundamental schematic of all three configurations is shown in Figure4.5.

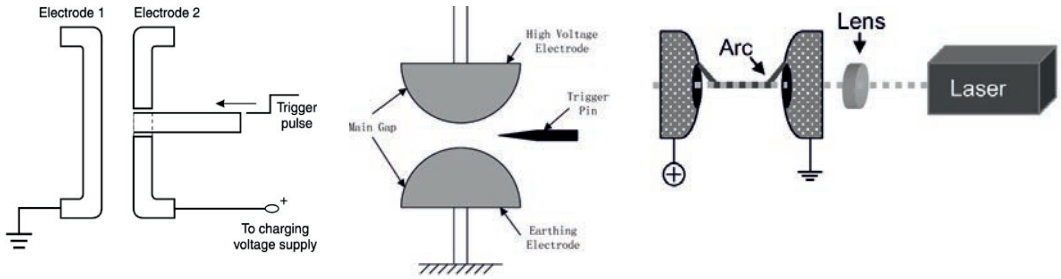

(a) Trigatron (b) Field distortion (c) Laser triggered

Figure 4.5. Schematic of three major configurations of sparkgap switches.

Of all configurations, the Trigatron type spark gap (Figure 4.5(a)) is the most compact, low cost and requires minimum maintenance. The main advantage of the Trigatron spark gap configuration is that it uses concentric trigger electrode and requires a relatively low trigger voltage to initiate a discharge within one of the main electrodes. The rise time of the trigger pulse is not critical and can range from <1 μs to tens of μs. Initial closure of the spark gap begins with a breakdown between the trigger electrode and the cathode, and this plasma expands further, creating an avalanche in the strong electric field region between the inter-electrode gaps, leading to switch closure. The major drawback with Trigatron switches is that they have high jitter and breakdown time delay due to inherent switch closure mechanism (i.e. by plasma expansion).

In Field distortion type of sparkgap switches (Figure 4.5(b)), a DC bias electrode is placed between the main electrodes so that the electric field is not altered. Breakdown in the inter-electrode gap region is initiated by applying a negative pulse to the trigger electrode, creating a heavily distorted electric field in inter-electrode gap region. Field distortion switches are best suited for applications where low jitter and low breakdown delay of switch is essential criteria. However it shall be noted that trigger pulse of large amplitude (in range of 30 to 50 kV) and high dV/dt (of ~5 to 10 kV/ns) is mandatory for attaining optimal performance of Field distortion switches.

The laser triggered sparkgap switches (Figure 4.5(c)) relies on light energy to vaporize part of the metal electrode. Hot metal vapor emits ultraviolet (UV) and this leads to production of free electrons on the electrode surface. Streamer is further heated by the applied electric field that reduces resistance and results in breakdown causing switch closure. Typically UV lasers with pulse energy of ~1 mJ of ~30 ns duration can reliably trigger this type of sparkgap

switch. It is remarkable to note that laser triggered sparkgap switches have jitter in sub-nanoseconds (i.e. as low as 50 ps).

Sparkgap switches of various configurations usually have maximum voltage hold-off and peak discharge current limit of about 100 kV/ 100 kA while the maximum charge transfer is limit to about 1 to 2 Coulomb per discharge.

4.3.2. Railgap Switch

Railgap switch is a specialized field distortion switch with extremely high current carrying capability and used in high energy capacitor banks to allow high charge transfer in spreaded manner. Railgap switch performance relies heavily on multi-channel breakdown between extended electrodes (rails) to ensure current transfer in distributed mode along the length of the electrodes and thus minimize switching inductance. The initiation of multiple arc channels along the electrode length depends on the trigger pulse characteristic that dictates the rate of change of the electric field in the gap [16]. The stringent requirement for trigger pulse include high speed slew rates above 5 kV/ns and high peak voltage well above the main gap operating voltage.

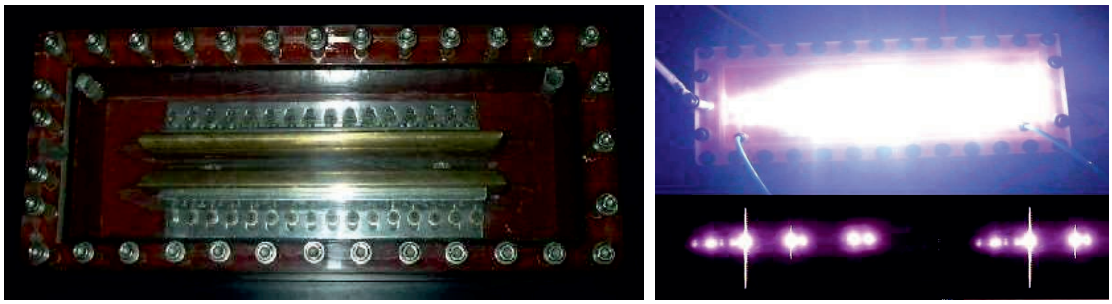

Figure 4.6. Railgap switch Maxwell #40200 and demonstration of multichannel discharge.

Railgap switches have maximum voltage hold-off and peak discharge current limit of about 120 kV/ 750 kA while the maximum charge transfer is limit up to 10 Coulomb per discharge. Jitter and switch inductance of railgap is typically ~2 ns and ~20 nH. Gas mixture of Ar-O_2 (85:15) and Ar-SF_6 (90:10) is commonly used for pressuringrailgap switches. Argon is being used as the prominent gas because of it supports multichannel formation owing to it low ionization potential (i.e. ~15.6 eV) and large ionization coefficient (i.e. ~30).

4.3.3. Pseudospark Switch

Pseudo-spark switches (PSGs) are low-voltage switching devices with cold cathodes, also known as copper arc thyratrons. Typical inductance of this switch is <20 nH and it can operate in repetitive mode up to 10 Hz. As with traditional hydrogen thyratrons, the

operating pressure range of the PSG switch lies on the vacuum side of the Paschen curve and the mean free path of electrons for ionization is well above the main electrode gap [17]. The PSG switch has a stacked ceramic metal structure and uses hydrogen in the range of 0.2 to 0.6 mbar. The trigger electrode is equipped with a special semiconductor discharge igniter. Figure 4.7 shows details of the appearance and structure of the TDI1150k / 25 Pseudo Spark Switch (Pulsed Technologies Ltd., made in Russia).

In PSG construction, parallel plate electrodes work as an anode and a cathode. Cathode is drilled axially to allow hydrogen gas in the anode-cathode gap region. Typical diameter of the hole is about 6 mm, which is comparable to the distance between the electrodes. Triggering of the switch requires an electron current to ignite the high current discharge. When pulsed trigger of appropriate voltage level is fed to igniter, emitted electrons pass through the cathode opening to the anode region and causes switch closure [18]. The device uses a heater to heat the hydrogen reservoir and release the working gas inside the switch and its pressure is controlled by adjusting the heater current. The PSG switch has low jitter (<5 ns) and stable breakdown characteristics, and the typical lifetime of this switch is approximately of 5×10^5 C (integrated charge transfer shot life). PSG switches have maximum voltage hold-off and peak discharge current limit of about 50 kV/ 200 kA while the maximum charge transfer is limit up to 5 Coulomb per discharge.

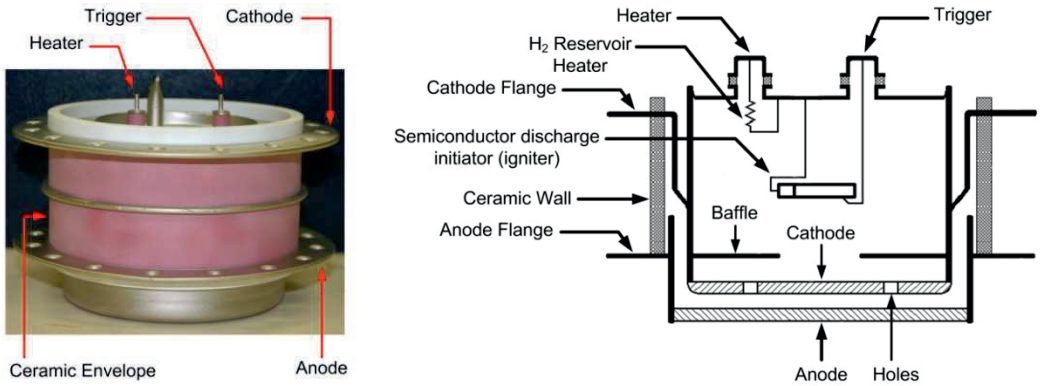

Figure 4.7. TDI1150k / 25 Pseudo-spark switch appearance and structural schematic.

4.3.4. Ignitron Switch

Ignitron is considered as a highly reliable switch with almost indestructible electrodes. The anode material is made up of Graphite or Molybdenum. An igniter is a small rod of semiconductor material partially immersed in a mercury pooled cathode [19]. Figure 4.8 shows the constructional view of an elementary ignitron switch and practical coaxial mounting of an NL8900 Ignitron switch that is most commonly used in several pulsed power systems. Squirrel cage configuration of current carrying conductors compensates the generated hoop stress generated during high pulsed current discharge. NL8900 ignitron switch has maximum voltage hold-off and peak discharge current limit of about 35 kV/ 300 kA

while the maximum charge transfer is limit up to 250 Coulomb per discharge. Specialty of NL8900 is that this model can be used in circuits that exhibit high voltage reversal.

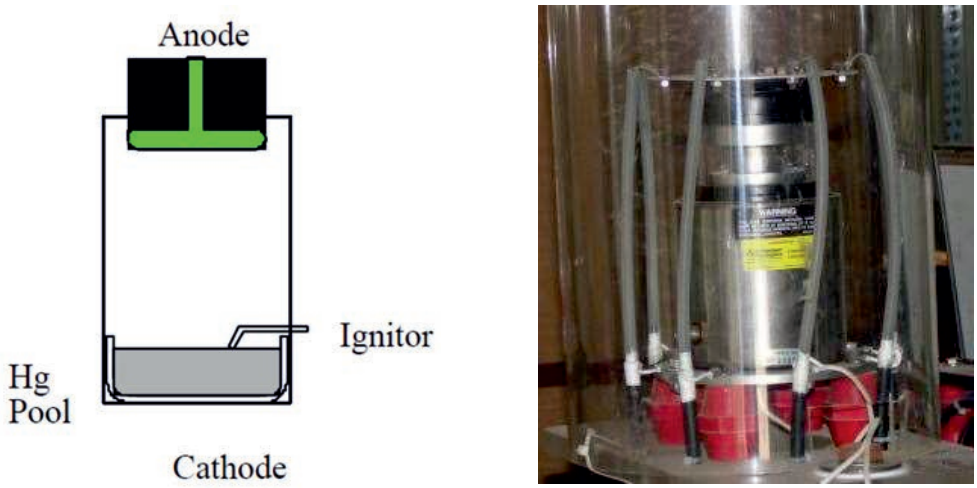

Figure 4.8. Constructional schematic of an elementary ignitron switch and coaxial mounting of NL8900 Ignitron switch having maximum ratings of 35 kV, 300 kA, 250 C.

This switch reliably withstands high voltage until any voltage is applied on igniter. A hotspot is formed when voltage is applied between the igniter and the mercury pooled cathode, causing the resistance to drop sharply from about 30 ohms to a few ohms and this leads to closing of the switch. In the conduction phase, the mercury pool cathode supplies unlimited number of electrons, making it ideal for controlled discharge of capacitor [19].

4.3.5. Moving-Arc Switch

Electro-dynamically accelerated spark channel based switch has been developed as an alternative to Ignitrons for high current and high coulomb transfer applications. The operating principle of this switch is based on the ability to move the established arc discharge by Lorentz force (J×B). The current flow between the two extended rails creates a magnetic field which generates force being exerted on the arc. Thus the electrical arc created at the closing-end of the switch runs along the electrodes along the two extended rail electrodes (as shown in Figure 4.9). The imposed displacement of the electrical arc limits the electrode erosion that dramatically increases switch lifetime [20]. In such a switch, the velocity spark and erosion of the electrodes is controlled by the diameter of the electrodes.

Figure 4.9. Schematic and actual operation of in-house developed moving-arc switch.

4.3.6. Solid-State Switches

In the recent period advancements in solid-state switches has improvised the performance of pulsed power systems by enhancing repetition rate, life-time, compactness, mobility, low cost and high efficiency. Various types of semiconductor switches like Thyristor, Bipolar Junction Transistor, MOSFET, IGBT and GTO are now commercial available is wide ratings and used in various applications. As each type of semiconductor switch has unique physical structure and operating characteristic, their peak power handling capacity and maximum frequency of operation varies accordingly. Relative comparison of power handling capacity and operating frequency of different types of semiconductor switches is depicted in Figure 4.10 [21].

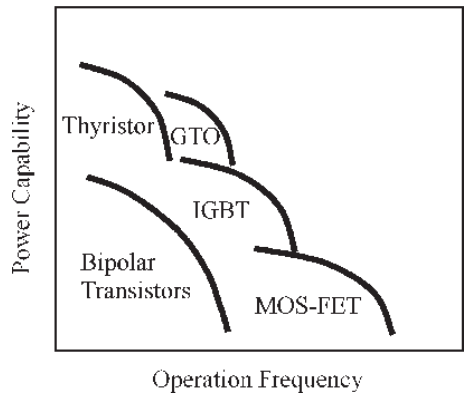

Figure 4.10. Schematic and actual operation of in-house developed moving-arc switch.

Amongst all solid-state switches Thyristor has maximum power handling capability but it operation frequency is typically limited to few 100's of Hz. The gate-turn-off (GTO) thyristor are also considered equivalent to Thyristor and they are rugged with simple control of gate drive. Bipolar transistors are used in relatively low power circuits as their power handling capacity and maximum operating frequency lies in moderate range. Insulated gate bipolar thyristor (IGBT) is the most popular and widely used solid-state switch having advantage of both high-power and high operating frequency (up to few 10's of kHz). Metal-oxide-

semiconductor field effect transistor (MOSFET) has best response amongst all and it is extensively used for high rep-rate up to MHz, however power handling capacity is limited up to few watts.

4.4. Charging Power Supplies

An important part of the hardware of a repetitive system is the charging power supply. It charges the capacitors in the specified time period. It shall be noted that the maximum rate of charging (PRF) is mainlygoverned by the peak power (Ppk) rating (J/s) of the charging power supply [22] and therefore, great care should be taken when choosing the rating of the HV charger to match the desired operating frequency. The sketch in Figure 4.11 shows a typical charge cycle of charging power supply (current is constant).

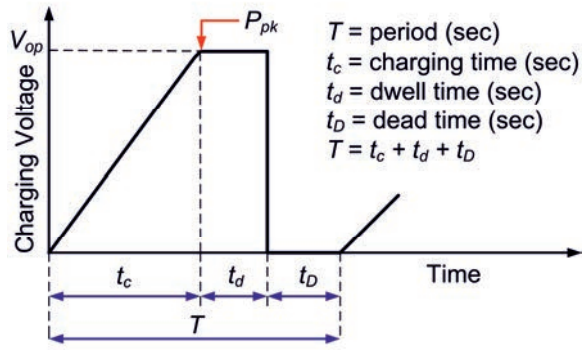

Figure 4.11. Charging cycle of a constant current power supply.

The charging profile shown in Figure 4.11 shows relation of charging voltage versus time. Here t_c is the charging time, t_d is the dwell time after which the capacitor is discharged and t_D is the dead time while charger is turned-off so that switch recovers fast. In repetitive applications, it is important to consider $t_{d,}$ $t_{D,}$ t_c . The charging time t_c (in seconds) may be calculated using the below relation [22]:

$$t_c = \frac{0.5 \times C_0 \times V_0 \times V_{rated}}{P_{pk}} \tag{4.18}$$

Here, $P_{pk}$is in Watts, C_o in Farads, V_{rated} is peak specified voltage of power supply in Volts and V_o is the charged voltage in Volts.

4.5. Hardware Integration

The mutual integration between 'capacitor-switch-load' is dictated by the magnitude of current and its discharge frequency required for the specific experiment. In fast banks with high discharge frequency, it becomes mandatory to limit the total inductance of the capacitor bank in the range of 50 nH to 100 nH. Practical approach adopted for minimizing the system inductance are: (i) switch is connected just above the capacitor output terminal in coaxial

arrangement and then multiple coaxial cables are connected at the switch output in parallel for delivering stored energy to load. In some cases, small loads may directly be interfaced as well in coaxial configuration and minimum inductance can be achieved. (ii) The second approach adopted is to connect multiple capacitors in parallel through a parallel plate transmission line and a single switch of sufficiently high rating is connected to collectively carry currents delivered by all capacitors. In this scheme, electrical connection between switch to load is done either by directly integrating load over the parallel plate transmission line of capacitor bank or by connecting multiple coaxial cables in parallel at the switch output extending up to load. Exemplary photographs of proposed integration is shown in Figure 4.12, where (a) represents direct integration of sparkgap switch over capacitor, (b) represents 4 nos. of energy storage capacitors connected in parallel through parallel plate transmission line directly interfaced to Railgap switch, (c) represents 8 nos. of energy storage capacitors connected in parallel through multiple coaxial cables and interfaced to coaxial mounted Ignitron switch, (d) represents a bipolar capacitor bank with 6 nos. of capacitors being fitted in parallel on each side through a common parallel plate transmission line and 2 Nos. of Railgap switches are connected in parallel over it. Load is also directly interfaced at the output side of Railgap and another end with the capacitors. No cables have been used in this bank.

(a)

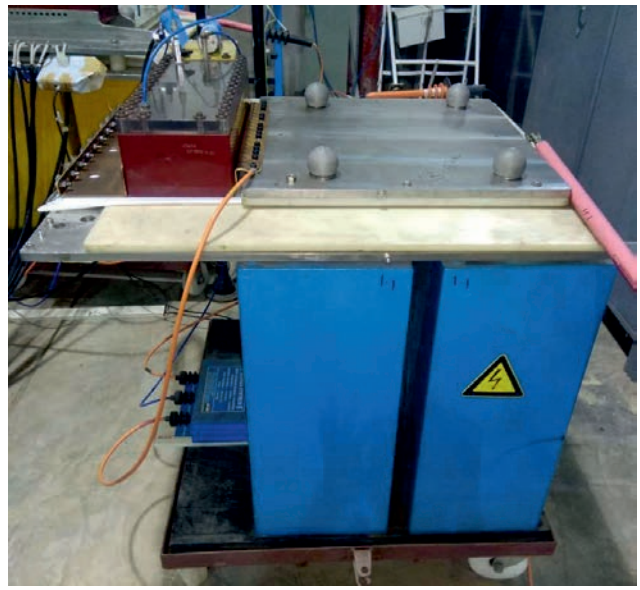

(b)

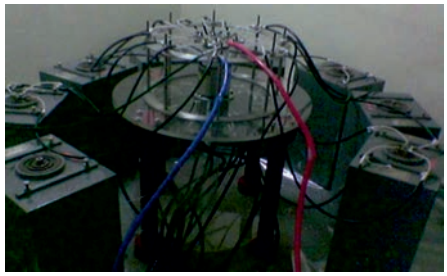

(c)

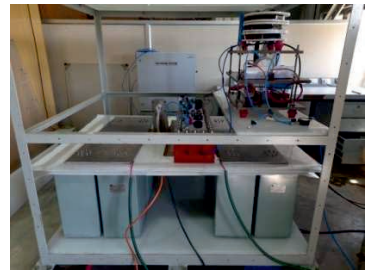

(d)

Figure 4.12. Various configurations of hardware integration of capacitor banks.

A major concern for high current, low inductance capacitor banks is the life expectancy of the energy transfer switch because discharge oscillates longer due to increased voltage reversal. It is important to note that at higher voltage reversal accelerated ion/electrons in both end of electrodes results in ablation of electrode material which may coat over dielectric spacer causing erratic trigger/ pre-firing of switch. There are two possible solutions for this problem (i) use one switch of highcharge exchange rating (ii) use multiple switches in parallel of low charge exchange capacity. Both schemes have their strengths and weaknesses. The prior choice greatly simplifies switching and trigger requirements and does not require very fast trigger pulse or high dV/dt) but the disadvantages are (a) switch inductance is high (b) due to the high charge transfer shot life of the switch is significantly reduced. In the second scheme, placing many switches in parallel has the advantage of reducing inductance and increasing lifetime, but for "synchronous discharge" high performance triggering (i.e. fast trigger pulse with high dV/dt) is required and multiple trigger pulses shall be generated and fed simultaneously to all parallel switches with minimum jitter. Sufficient measures are also required to prevent energy exchange between modules and therefore careful selection of appropriate scheme is required.

4.6. Interconnections

As shown in the pictures of the various systems in Figure 4.12, for connecting capacitor to switch and switch to the load either parallel coaxial cables or flat transmission line may be used.In large capacitor banks with several discharge modules, it is advantageous to use coaxial cables because its parallelization reduces inductance and flexibility in choosing appropriate length helps in easily adjusting the ‘transit time isolation’ between the modules. The outer braid covering in coaxial cable also helps in reducing the electromagnetic noise. Although there are many advantages to using coaxial cable along with its flexibility but the inductance of this class of coaxial cables (eg RG213, URM 67 and RG218) is typically ~250 nH/m, hence usage of large number of cables in parallel is must requirement. Flat plate transmission lines have advantages over coaxial cables in the following ways: (a) connections to capacitors and discharge switches are convenient with high reliability, (b) reduced size and complexity of the system, and (c) greater economy and durability. However, there are two

main limitations (i) transit time decoupling is practically nil because of the size of the flat plate and (ii) the flexibility to hold the load in any orientation gets very limited. Therefore, based on the above considerations, both parallel plate transmission line and coaxial cable schemes should be appropriately chosen depending upon load and application requirement. As shown in Figure 12(b) and 12(d), for connecting the capacitors in modular fashion, parallel plate transmission line configuration has been used. The inductance (L_T) of parallel plates with dielectric separation in between is estimated as:

$$L_T = \mu_0 \frac{d}{W} \; Henry/meter \tag{4.19}$$

As evident from Eq. (19), the clearance between the plates $d$must be as small as possible (much lower than the width W of plate) and the dielectric strength of spacer materials shall also be in good range.

4.7. Summary

High current fast capacitor banks are the main workhorse for conducting wide range of pulsed power experiments and applications and distinct demand of peak current magnitude and discharge frequency compels designers for the judicious selection of type's capacitors and their ratings, appropriate type of switches and their ratings and finally the hardware integration and interconnection approach. All these aspects are comprehensively discussed and methodically addressed in this chapter for giving a detailed overview and major considerations to be accounted by practicing pulsed power engineers while designing a high current capacitor bank.

References

[1] JMMVS Aravind, S. Mishra, S. K. Sharma, P. Dey, R. Verma, R. Shukla, E. Mishra and Archana Sharma, Generation and measurement of high tesla magnetic field with single turn destructible coil, 16th International Conference on Megagauss magnetic field generation and related topics (MG-XVI), 25-29 Sep 2018, University of Tokyo, Japan.

[2] Y. Okuda, S. H. R. Hosseini, D. Oshita, S. Iwasaki, T. Sakugawa, H. Akiyama, Production of uniform underwater shock waves by pulsed electric discharge, IEEE Pulsed Power Conference, 19-23 June 2011, Chicago, IL, USA.

[3] Rishi Verma, Ekansh Mishra, ProsenjitDhang, Basanta Kumar Das, ManrajMeena, LakhsmanRongali and Archana Sharma, Development and performance characterization of compact plasma focus based portable fast neutron generator, Plasma Science and Technology, **22 (11)** 115506 (2020).

[4] H.G. Haines, A review of the dense Z-pinch, Plasma Phys. Control. Fusion, **53** (2011), 093001.

[5] S.G. Tatake, K.J. Daniel, K.R. Rao, A.A. Ghosh, and I.I. Khan, Railgun, Defence Science Journal, **44(3)**, July 1994, pp 257-262.

[6] F. MacDougall, T. R. Jow, J. Ennis, S.P. S. Yen, X. H. Yang, J. Ho, Pulsed Power Capacitors, IEEE Power Modulator Conference, May 2008.

[7] http://home.earthlink.net/~jimlux/hv/caplife.htm.

[8] http://www.gaep.com/tech-bulletins/voltage-reversal.pdf

[9] http://www.highvoltageprobes.com/PDF/formweb1.pdf

[10] R. E. Beverly III and R. N. Campbell, Transverse-flow 50-kV Trigatron switch for 100-pps burst-mode operation, Rev. Sci. Instrum.,**67** 1593 (1996).

[11] P. H. Ron, K. Nanu, S. T. Iyenger, K. V. Nagesh, R. K. Rajawat and V. R. Jujaray, An 85kJ high performance capacitor bank with double mode Trigatron, Rev. Sci. Instrum., 63 37 (1992).

[12] T. Y. Tou, K. S. Low and B. C. Tan, A simple two-stage cascading spark gap for ultraviolet preionized transversely excited atmospheric CO2 lasers, Rev. Sci. Instrum.,**62**2584(1991).

[13] F. E. Peterkin and P. F. Williams, *Physica1 mechanism of. Triggering in Trigatron Spark Gaps*, Appl. Phys. Lett.,**53** 13 (1988).

[14] J. M.Buzzi, H. J.Doucet, W. D. Jones, H.Lamain and C. Rouille, *A very-low-inductance triggered multichannel surface switch*,Rev. Sci. Instrum.,**61**852 (1990).

[15] I. H. Mitchell, P. Choi, J. M.Bayley, J. P. Chittenden and J. F. Worley, *Optimization of a high-voltage trigatron switch, J. Appl. Phys.,* **78**3659(1995).

[16] K. Masugata, H. Tsuchida, H. Saitou and K. Yatsui, Studies and performance of decreased railgap switch inductance by enhancing multichanneling via gas mixture, IEEE transactions on Plasma Science, **25** (1), pp. 97 – 99, (1997).

[17] V. A. Gribkov, M. Scholz, V. D. Bochkov, A. V. Dubrovsky, R. Miklaszewski, L. Karpinski, P. Strzyzewski, P. Lee and S. Lee,Pseudosparks in the nanosecond range of operation: firing, jitter, and current disruption, *J. Phys. D: Appl. Phys.,* 37 2107 (*2004).*

[18] *E. P. Bogolyubov, V. D. Bochkov, V. A. Veretennikov, L. T. Vekhoreva, V. A. Gribkov, A. V. Dubrovskii, Yu. P. Ivanov, A. I. Isakov, O. N. Krokhin, P. Lee, S. Lee, V. Ya. Nikulin, A. Serban, P. V. Silin, X. Feng and G. X. Zhang,*A powerful soft x-ray source for x-ray lithography based on plasma focusing, *Phys. Scr.* ***57*** *488 (1998).*

[19] http://www.relltubes.com/products/High-Energy-Transfer-Products/Ignitron.html

[20] B. M. Kovalchuk, A. A. Kim, A. V. Kharlova), E. V. Kumpyak, N. V. Tsoy, V. V. Vizir, and V. B. Zorin, *Three-electrode gas switches with electrodynamical acceleration of a discharge channel,* Review of Scientific Instruments 79, 053504 (2008).

[21] Weihua Jiang, Kiyoshi Yatsui, Ken Takayama, M. Akemoto, EijiNakamura, N. Shimizu, Akira Tokuchi, Sergei Rukin, Victor Tarasenko, Alexei Panchenko, *Compact solid-State switched pulsed power and its applications*, Proceedings of the IEEE (2004),**92,** 1180 - 1196.

[22] http://www.us.tdk-lambda.com/hp/pdfs/application%20notes/93008500rC.pdf.